Accepted Manuscript

A Novel Training-free Method for Real-time Prediction of Femoral Strain

Hamed Ziaeipoor, Mark Taylor, Marcus Pandy, Saulo Martelli

PII: S0021-9290(19)30116-2
DOI: https://doi.org/10.1016/j.jbiomech.2019.01.057
Reference: BM 9066

To appear in: *Journal of Biomechanics*

Received Date: 26 September 2018
Revised Date: 28 December 2018
Accepted Date: 30 January 2019

A Novel Training-free Method for Real-time Prediction of Femoral Strain

*Hamed Ziaeipoor [a], Mark Taylor [a], Marcus Pandy [b], Saulo Martelli [a]

[a] Medical Device Research Institute, College of Science and Engineering,

Flinders University, Clovelly Park, SA, Australia

[b] Department of Mechanical Engineering, University of Melbourne, Parkville, VIC, Australia

To be submitted as a Full-Length Article to Journal of Biomechanics

*Corresponding author

Hamed Ziaeipoor

PhD Student,

Medical Devices Research Institute, College of Science and Engineering

Flinders University, Clovelly Park, Adelaide, SA, Australia

Telephone +61 8 8201 5732

Mobile: +61 410 009 029

Email: hamed.ziaeipoor@flinders.edu.au

Abstract:

Surrogate methods for rapid calculation of femoral strain are limited by the scope of the training data. We compared a newly developed training-free method based on the superposition principle (Superposition Principle Method, SPM) and popular surrogate methods for calculating femoral strain during activity. Finite-element calculations of femoral strain, muscle, and joint forces for five different activity types were obtained previously. Multi-linear regression, multivariate adaptive regression splines, and Gaussian process were trained for 50, 100, 200, and 300 random samples generated using Latin Hypercube (LH) and Design of Experiment (DOE) sampling. The SPM method used weighted linear combinations of 173 activity-independent finite-element analyses accounting for each muscle and hip contact force. Across the surrogate methods, we found that 200 DOE samples consistently provided low error (RMSE < 100 με), with model construction time ranging from 3.8 to 63.3 hours and prediction time ranging from 6 to 1236 seconds per activity. The SPM method provided the lowest error (RMSE = 40 με), the fastest model construction time (3.2 h) and the second fastest prediction time per activity (36 s) after Multi-linear Regression (6 s). The SPM method will enable large numerical studies of femoral strain and will narrow the gap between bone strain prediction and real-time clinical applications.

Keywords: Surrogate methods; Superposition principle method; Finite element analysis; Physical activity; Musculoskeletal modelling.

Introduction

Quantifying femoral strain in real time or near-real time is important for different biomechanical applications such as predicting femoral strains over multiple activities and trials (Martelli et al., 2015b; Phillips et al., 2015), in statistical studies using hundreds (Martelli et al., 2015c) to thousands of loading cases (Martelli et al., 2015a), and providing biofeedback to patients while exercising (Pizzolato et al., 2017). Over the last 40 years, finite-element analysis has been shown to be a powerful tool for predicting femoral strains (Taylor and Prendergast, 2015). However, building the model, generating a solution, and interpreting the results are time- and labour-intensive (Liang et al., 2018; Panagiotopoulou et al., 2014). There are several bottlenecks in the process, including generating the model from clinical images through to the solution phase. Various groups have developed methods to rapidly segment and generate the finite element models from CT scans (Carballido et al., 2015; Pauchard et al., 2016; Younes et al., 2014). The next major bottleneck is the solution phase.

To reduce the computational cost of finite-element analyses, several surrogate methods have been used in computational biomechanics, including Artificial Neural Networks (Cilla et al., 2017; Eskinazi and Fregly, 2015; Taylor et al., 2017), Multi-linear Regression (Fitzpatrick et al., 2014), Multivariate Adaptive Regression Splines (Friedman and Roosen, 1995; Wang et al., 2014), Kriging (O'Rourke et al., 2016; Walter and Pandy, 2017) and Gaussian process modelling (Seeger, 2004). Multivariate Adaptive Regression Splines is an extension of the multi-linear regression method, which can be used to model the nonlinearities between variables by partitioning the training datasets into separate linear or cubic splines known as ‘basis functions’ (Friedman and Roosen, 1995). Gaussian process modelling, which provides a trade-off between fitting the data and smoothing, can handle noisy training datasets while capturing the precise trend of the data (Wang and Shan, 2007). Artificial Neural Networks provide an effective solution when the optimum number of artificial neurons needed for building the network structure can be determined *a priori*, for example, using trial-and-error approaches (Cilla et al., 2017; Tu, 1996). Kriging is best suited for nonlinear problems, but typically requires large training sets and is computationally expensive (Eskinazi and Fregly, 2015). Therefore, Multi-linear Regression (MLR), Multivariate Adaptive Regression Splines (MARS), and Gaussian process (GP) methods appear to be the best suited for predicting femoral strain during activity. However, the performance of each surrogate model is application-dependent and bounded by the scope of training data (Forrester and Keane, 2009; Jin et al., 2001). For example, a surrogate model trained on data for level walking is unlikely to be as effective in predicting musculoskeletal loading patterns for activities with a higher degree of variability such as stumbling and jumping.

By leveraging the linearity of most models used to predict femoral strain (Fitzpatrick et al., 2014; Liang et al., 2018; Martelli et al., 2014), the superposition principle can provide a solution that may outperform current surrogate methods while being applicable to every possible motor task or activity, without training. In the most general case, a muscle's contribution to femoral strain can be described by calculating the strain tensor generated by three independent nominal force vectors applied to each of the muscle's attachment points, and is therefore not related to a specific frame of motion. The displacement of the joint contact area during motion can be modelled by discretising the patch on the joint surface spanned by the joint contact force into a finite number of nodes. The strain tensor generated by the hip contact force can then be described by calculating the strain tensor generated by three independent nominal force vectors applied to each node in the patch. Femoral strain for a given frame of motion can be calculated by (1) matching the centre of pressure for the specific frame of motion using, for example, musculoskeletal modelling, and (2) determining the weights for the strain tensor generated by each nominal force component as the ratio between the amplitude of the actual force component and that of the nominal force applied. This model, henceforth referred to as the Superposition Principle Method (SPM), does not require training, and can be generated independently from motion analyses experiments.

The aim of the present study was to develop an SPM model for one representative individual and to compare its performance to that of MLR, MARS, and GP for the prediction of femoral strain for a range of activities and trials. Motion data and a finite-element model of the right femur for one healthy volunteer were obtained from a previous study (Ziaeipoor et al., 2018) to calculate the femoral strain as the reference. The strain error and the CPU time required for solving the elastic problem of the femur by SPM, MLR, MARS, and GP methods were computed and compared. We hypothesized that the Superposition Principle Model (SPM) would outperform popular surrogate methods for the calculation of femoral strain during activity in relation to both accuracy and total computational time required.

Methods

Muscle and joint forces and femoral strain during activity

Muscle and joint reaction forces and the femoral strain field were calculated previously for one healthy participant (68 years of age, 53 kg weight, 157 cm height) executing five different tasks (Ziaeipoor et al., 2018). Marker-trajectory and ground-reaction-force data were obtained for normal walking (5 trials), fast walking (5 trials), stair ascent (4 trials), stair descent (4 trials) and chair sitting (1 trial). The full-body 12-segment musculoskeletal model actuated by 92 Hill-type muscle–tendon units proposed by Delp et al. (2007) was scaled to the participant mass and anthropometry using measurements of body weight and segment lengths acquired during a static trial (Figure1). Dynamic simulations were performed using OpenSim to calculate muscle and joint forces for 50 uniformly distributed frames across each trial. The muscle and joint reaction forces calculated at each time frame were applied to a finite-element model of a femur using a custom routine (Martelli et al., 2015b). Joint angles, muscle forces and joint reaction forces were computed using the inverse kinematics, static optimization, and joint reaction analysis tools available in OpenSim (Delp et al., 2007). The finite-element model of the femur was a locally isotropic, unstructured mesh consisting of 213,559 nodes and 143,534 elements that was fully constrained distally (Figure 1). The geometry and locally-isotropic material properties of the mesh were obtained from a previous study (Martelli et al., 2015b) using calibrated computed-tomography images and a published bone density to Young modulus relationship (Morgan et al., 2003). Details of this procedure are given by Schileo et al. (2007). The femur model was fully constrained distally to satisfy equilibrium according to earlier studies (Behrens et al., 2009; Zhou et al., 2017). The equivalent strain at the element centroid was computed using the linear-elastic solver implemented in Abaqus (Dassault Systems, USA). Thus, the full dataset comprised of muscle and joint reaction forces and femoral strains for 1000 frames (50 frames per trial for 20 trials, in total).

Surrogate methods

Two sampling methods, Latin Hypercube (LH) and Design of Experiment (DOE), were used to generate training sets from the original data. Latin Hypercube provided random samples while DOE provided samples that best spanned the variation in the original data (Giunta et al., 2003). Training datasets of four different sizes (i.e., 50, 100, 200, and 300) required for developing MARS and GP methods were obtained for each mesh element and MLR was trained by taking the data from our earlier work (Ziaeipoor et al., 2018). All surrogate methods were implemented using custom code in Matlab (The Mathworks Inc., Natick, USA).

Superposition principle model

A new method termed the Superposition Principle Model (SPM) was developed by leveraging the load-strain linear response in common finite-element models ensuring that every solution in the model can be expressed as a linear combination of a base of independent solutions. The SPM model was essentially a look-up table composed by a set of strain fields generated by nominal force vectors, each arbitrarily set to 100 N, applied to each muscle attachment and application point of the hip contact force. Finally, the strain tensor during a generic frame of motion was calculated as the sum of strain fields in the look-up table weighted by the ratio between the force intensity provided by the OpenSim model and the nominal force intensity (100 N).

For the 24 muscles in the model acting on the femur, the femoral strain in the look-up table was calculated by applying the nominal force along each of the three coordinate axes for each of the 24 muscle-attachment sites, resulting in 72 strain fields.

The displacement on the hip centre of pressure during movement was modelled by identifying the node patch on the femoral head spanned by the hip centre of pressure. The centre of pressure was assumed to be the intersection between the sphere that best fit the femoral head surface (i.e., the hip centre henceforth) and the hip contact force vector passing through the hip joint centre. The patch was composed by 101 nodes within the envelope of the trajectories of the hip joint centre of pressure across activities. For each node in the patch, the SPM model was completed by the strain field calculated using a nominal force vector $\overrightarrow{hf}v_z$ pointing to the hip joint centre. This condition represents a frictionless ball and socket joint consistent with a very low coefficient of friction characterising natural joints (Pawlak et al., 2015).

The total strain tensor $\overline{\overline{\varepsilon_i}}$ generated by both muscle and hip contact forces for a generic frame i of activity was given by:

$$\bar{\bar{\varepsilon}}_i = \sum_{j=1}^{24} \sum_{k=1}^{3} \frac{fm_{i,j,k}}{f_n} \times \bar{\bar{\varepsilon}}(fv_{j,k}) + \frac{fh_i}{f_n} \times \bar{\bar{\varepsilon}}(\overrightarrow{hf}v_{i,z}), \qquad \text{Eq. 1}$$

where $fm_{i,j,k}$ is the magnitude of the force component *k*, muscle *j*, frame *i*, obtained using models of human motion (Martelli et al., 2015b); $\bar{\bar{\varepsilon}}(fv_{j,k})$ is the strain tensor generated by a nominal force *fn* applied at the muscle attachment point *j* along the coordinate axis *k*; fh_i is the magnitude of the hip contact force obtained using models of human motion (Martelli et al., 2015b) for frame *i;* and the nominal strain tensor $\bar{\bar{\varepsilon}}(\overrightarrow{hf}v_{i,z})$ was generated by a force vector $\overrightarrow{hf}v_z$ of magnitude *fn* applied to the node *z* at the femoral head surface. The node index *z* was dynamically determined by best matching the orientation of the hip contact force in the musculoskeletal model and that of the force $\overrightarrow{hf}v_z$.

Assessment of performance

The equivalent von Mises strain was calculated from the predicted strain tensor $\bar{\bar{\varepsilon}}_i$ to provide a compact assessment of the models' performance relevant to both tensile and compressive states. The strain error was calculated as the difference between the strain predicted by the surrogate and SPM methods and corresponding finite-element calculations of strains. For each surrogate method studied, the sample size and sampling method providing minimal strain error were identified. Surrogate and SPM models were compared using linear regression. The strain error was assessed at three levels: by pooling all the activities and trials together; activity-by-activity by amalgamating all the trials of each activity; and frame-by-frame. The Root Mean Square Error (RMSE) and 95th percentile of the strain error distribution were used as indicators of mean and peak error. The coefficient of determination (R^2) and slope were used as indicators of goodness of fit. To gain insight into the source of error in the SPM method, the contribution to the total strain error in the SPM model of each muscle force and joint reaction force was calculated separately. Model efficiency was assessed using a standard desktop computer (Intel Core i7 processor, 8 CPUs, 32 GB RAM). Total CPU time included the time required for constructing the models, the time needed to execute the FE simulations in the training set, and the training time. The time required for predicting strain during an entire activity (50 frames) and the total time required for predicting strain for all the 1000 frames, including both model construction and prediction, were also compared.

Results

The DOE sampling method was superior to the LH method for each training sample size, with both methods showing only a marginal improvement in the mean and peak errors above 200 training samples (Table 1). Specifically, RMSE varied from 134 με to 99 με, 187 με to 100 με, and 91 με to 53 με for MLR, MARS, and GP, respectively, when 200 training samples were used. RMSE improved on average by less than 10 με when the training sample size was increased to 300 samples. Peak error obtained for the MLR method with 200 training samples remained less than 521 με, thus assessment of the performance of MLR, MARS and GP was based on the DOE method with a training sample size of 200 (Table 1).

Overall, SPM was found to be the most effective, showing the lowest mean (RMSE = 40 με) and peak (PE = 256 με) errors. By comparison, mean errors were 99, 100, 53 με while peak errors were 521, 414, 316 με for MLR, MARS and GP, respectively. Across activities, the strain error remained relatively constant showing a peak error consistently below 300 με for all methods, except when MLR and MARS were applied to the chair rise task, where the peak error was higher than 350 με. SPM performed best for the chair rise task (RMSE = 6 με; PE = 47 με) and showed similar performance to that of GP for the remaining activities (RMSE < 30 με; PE < 172 με) (Figure 2).

Comparing the performance of SPM and GP within a given activity, both models predicted femoral strains that were highly correlated to results obtained from corresponding finite-element calculations. The coefficient of determination (R^2) was 0.97 – 1.00 for SPM and 0.88 – 0.99 for GP. The slope of the linear regression was 0.96 – 1.08 for SPM and 0.83 – 1.04 for GP. The GP model showed higher mean and peak errors during early and late stance, reaching 153 με and 380 με, respectively, during late stance (Figure 3). The SPM model showed mean and peak errors of 0 – 96 με and 0 – 257 με, respectively, and presented a pattern across the different frames not visibly related to a specific gait phase (Figure 3). The strain error distribution was located for the most part in the distal femur for both SPM and GP (Figure 4). The strain error measured for SPM was entirely associated with the hip contact force and zero error was observed for all muscle forces.

The SPM model provided the fastest construction time and the second fastest prediction time (Figure 5). Constructing the SPM model took 3.2 hours for solving 173 finite-element simulations. Constructing the surrogate methods took 3.66 hours for solving the 200 finite-element analyses in the training set and 0.15, 59.7 and 0.8 hours for training MLR, MARS, and GP, respectively. Predicting the femoral strain for an entire activity (50 frames) took approximately 36 s for SPM, and 6 s, 357 s and 1236 s for MLR, MARS, and GP, respectively.

When comparing the total time required by SPM, MLR, MARS, GP and a full finite-element analysis for predicting femoral strain for an increasing number of frames, SPM showed the fastest prediction time for all 1000 frames (3.4 hours) and outperformed a full finite-element analysis when 176 frames or more were analysed. MARS and GP always underperformed SPM due to a greater amount of time required for constructing the model and predicting strain whereas the number of frames above which the MLR model outperformed the SPM model was 3660 (Figure 5).

Discussion

We developed a superposition principle model (SPM) and compared its performance to that of multi-linear regression (MLR), multivariate adaptive regression splines (MARS) and Gaussian process (GP) for estimating the full-field strain in one human femur across a range of daily activities. The SPM model did not require training and showed the highest accuracy, the lowest total time for predicting femoral strain for all 1000 frames studied, the lowest model construction time, the lowest number of frames above which it outperformed corresponding full finite-element analyses, and the second-fastest prediction time relative to the MLR method. Thus, the SPM method offers a training-free approach while providing the highest accuracy and lowest prediction time for most foreseeable biomechanical applications.

The models studied for fast prediction of femoral strain produced an average strain error (RMSE = 40 – 100 με) over corresponding finite-element calculations that is comparable to the average strain error in current finite-element models (RMSE = 113 με; Schileo et al. (2007)) hence supporting the use of SPM, MLR, MARS and GP models as valid alternatives to full finite-element analyses. Among the models analysed in the present study, SPM showed the lowest error (RMSE = 40 με), the fastest model generation time (3.2 hours), and the second-fastest prediction time per activity (36 s) after MLR (6 s), supporting the SPM method as a valid alternative for biomechanical applications requiring fast strain prediction time. The MLR method may outperform SPM when several thousands of loading cases are examined.

Differently from surrogate models, the SPM model can be developed independently from muscle and joint force analyses and later used to analyse any activity and without training, which incurs a high computational cost when developing a surrogate method. Therefore, SPM is a training-free method not bounded by the scope of the available motion data, often obtained by combining motion experiments and musculoskeletal modelling. Also, SPM provides the strain parameter of interest, i.e., the von Mises strain in the present study, through calculation of the full strain tensor, while surrogate methods are trained separately for each parameter in output. While this may explain the slower prediction time of SPM compared to MLR, the difference in the computational cost between these two methods decreases when multiple strain parameters are of interest.

Another difference between SPM and surrogate methods concerns the origin of error. The SPM error reported here originated completely from the different algorithm used in the present study for defining the node of application of the hip contact force and that in the study of reference (Martelli et al., 2015b). Specifically, in the present study the node of application of the hip contact force was determined by matching the direction of the hip contact force vector calculated using OpenSim and the direction passing through the node and the hip centre whereas, in the study of reference, the node of application of the hip contact force was the node on the femoral head surface closest to the intersection between the hip contact force vector calculated using OpenSim and the femoral head surface. The different algorithms led to a mismatch between the point of application of the hip contact force in the two studies of up to the element edge length (2 mm in average) and to zero-error when the hip force vector was applied to the same node in both studies. Thus, the accuracy of the SPM method can be improved using a smaller element size while the accuracy of surrogate methods can only be moderately improved by increasing the training set size above 200 (Table 1).

Confidence in the validity and reliability of the present results may be gained through a comparison with previous studies. For example, the size of the training set in the present work is in agreement with earlier studies that used 100 – 200 samples for training a MLR method (Fitzpatrick et al., 2014), 200 – 500 samples for training an Artificial Neural Network (Taylor et al., 2017) and 300 samples for training a Kriging-based method (O'Rourke et al., 2016). Also, and in agreement with earlier studies (Giunta et al., 2003; Wang et al., 2014), we found that DOE sampling systematically reduces both the mean and peak errors for all methods, particularly MARS (Table 1), as a broader distribution of samples is generated. These observations support the validity of the surrogate methods developed here. The principle of superposition has been long used in musculoskeletal modelling studies for determining the contribution of individual muscles to joint motion and loading, commonly referred to as muscle-induced acceleration analysis (Kersh et al., 2018; Pandy, 2001; Pandy and Zajac, 1991). The present study applies the same principle to the strain tensor in the human femur by combining the strain tensor generated by each separate force applied to the model rather than fitting the data by training a surrogate model. Therefore, SPM is better suited than surrogate models for studying the causal relationships between muscle force, joint contact force and femoral strain.

One limitation of the present study is that the time required for predicting strain for the 50 frames of an entire activity (i.e., 36 s for SPM and 6 s for MLR) was higher than the real-time duration of normal activities. Truly real-time analyses may be possible using alternative programming languages such as C++ or Fortran (Aruoba and Fernández, 2015) and/or by determining the optimal mesh size and frame rate for the desired model accuracy and speed. A second limitation is that the SPM method was developed for an intact femur and may not outperform other surrogate models when highly non-linear problems such as joint replacement models and material non-linearity are of interest. Other surrogate methods might be better suited for addressing these types of problems. Finally, the SPM model was developed for one single femur, which may limit generality of the conclusions. However, the SPM method presented here can be generally applied to every linear-elastic and non-linear contact problem. Furthermore, the large range of loading conditions spanned by each model, separately generated for each element in the mesh, across a range of normal activities provides confidence on the SPM method’s superiority over alternative surrogate methods.

Conclusion

In summary, we developed a Superposition Principle Method (SPM) for rapid prediction of femoral strain by leveraging the linear properties of common finite-element models of femoral strain and compared its performance to that of surrogate models, including MLR, MARS and GP. SPM required the lowest model generation time and provided the highest accuracy, the fastest total prediction time for all 1000 frames of motion studied, the second-fastest prediction time per activity, and did not require training. Thus, SPM offers the best performance among surrogate methods in predicting femoral strains over multiple activities and trials, in statistical studies using hundreds to thousands of loading cases and, in clinical trials, where, for example, biofeedback is used in rehabilitation exercise. MLR may be advantageous when several thousands of loading conditions are examined.

Ethics

Not required.

Conflict of interest statement

We have no competing interests.

Acknowledgements

This work was supported by the Australian Government Research Training Program Scholarship (AGRTPS) for Mr. Hamed Ziaeipoor and the Australian Research Council [DP180103146, FT180100338].

References

Aruoba, S.B., Fernandez, V., J., 2015. A comparison of programming languages in macroeconomics. Journal of Economic Dynamics and Control 58, 265-273. doi:10.1016/j.jedc.2015.05.009

Behrens, B.A., Nolte, I., Wefstaedt, P., Stukenborg-Colsman, C., Bouguecha, A., 2009. Numerical investigations on the strain-adaptive bone remodelling in the periprosthetic femur: Influence of the boundary conditions. Biomedical Engineering 8. doi:10.1186/1475-925x-8-7

Carballido, G.J., Bonaretti, S., Saeed, I., Harnish, R., Recker, R., Burghardt, A.J., Keyak, J.H., Harris, T., Khosla, S., Lang, T.F., 2015. Automatic multi-parametric quantification of the proximal femur with quantitative computed tomography. Quantitative Imaging in Medicine and Surgery 5, 552-568. doi: 10.3978/j.issn.2223-4292.2015.08.02

Cilla, M., Borgiani, E., Martínez, J., Duda, G.N., Checa, S., 2017. Machine learning techniques for the optimization of joint replacements: Application to a short-stem hip implant. Plos One 12. doi:10.1371/journal.pone.0183755

Delp, S.L., Anderson, F.C., Arnold, A.S., Loan, P., Habib, A., John, C.T., Guendelman, E., Thelen, D.G., 2007. OpenSim: open-source software to create and analyze dynamic simulations of movement. IEEE Transactions on Biomedical Engineering 54, 1940-1950.

Eskinazi, I., Fregly, B.J., 2015. Surrogate modeling of deformable joint contact using artificial neural networks. Medical Engineering & Physics 37, 885-891. doi:10.1016/j.medengphy.2015.06.006

Fitzpatrick, C.K., Hemelaar, P., Taylor, M., 2014. Computationally efficient prediction of bone–implant interface micromotion of a cementless tibial tray during gait. Journal of Biomechanics 47, 1718-1726. doi:10.1016/j.jbiomech.2014.02.018

Forrester, A.I., Keane, A.J., 2009. Recent advances in surrogate-based optimization. Progress in Aerospace Sciences 45, 50-79. doi:10.1016/j.paerosci.2008.11.001

Friedman, J.H., Roosen, C.B., 1995. An introduction to multivariate adaptive regression splines. Statistical Methods in Medical Research 4, 197-217. doi:10.1177/096228029500400303

Giunta, A., Wojtkiewicz, S., Eldred, M., 2003. Overview of modern design of experiments methods for computational simulations. 41st Aerospace Sciences Meeting and Exhibit. doi:10.2514/6.2003-649

Jin, R., Chen, W., Simpson, T., 2001. Comparative studies of metamodelling techniques under multiple modelling criteria. Structural and Multidisciplinary Optimization 23, 1-13. doi:10.1007/s00158-001-0160-4

Kersh, M.E., Martelli, S., Zebaze, R., Seeman, E., Pandy, M.G., 2018. Mechanical loading of the femoral neck in human locomotion. Journal of Bone and Mineral Research 33, 1999-2006. doi:10.1002/jbmr.3529

Liang, L., Liu, M., Martin, C., Sun, W., 2018. A deep learning approach to estimate stress distribution: a fast and accurate surrogate of finite-element analysis. Journal of the Royal Society Interface 15, 20170844. doi:10.1098/rsif.2017.0844

Martelli, S., Kersh, M.E., Schache, A.G., Pandy, M.G., 2014. Strain energy in the femoral neck during exercise. Journal of Biomechanics 47, 1784-1791. doi:10.1016/j.jbiomech.2014.03.036

Martelli, S., Calvetti, D., Somersalo, E., Viceconti, M., 2015a. Stochastic modelling of muscle recruitment during activity. Interface Focus 5, 20140094. doi:10.1098/rsfs.2014.0094

Martelli, S., Kersh, M.E., Pandy, M.G., 2015b. Sensitivity of femoral strain calculations to anatomical scaling errors in musculoskeletal models of movement. Journal of Biomechanics 48, 3606-3615. doi:10.1016/j.jbiomech.2015.08.001

Martelli, S., Valente, G., Viceconti, M., Taddei, F., 2015c. Sensitivity of a subject-specific musculoskeletal model to the uncertainties on the joint axes location. Computer Methods in Biomechanics and Biomedical Engineering 18, 1555-1563. doi:10.1080/10255842.2014.930134

Morgan, E.F., Bayraktar, H.H., Keaveny, T.M., 2003. Trabecular bone modulus-density relationships depend on anatomic site. Journal of Biomechanics 36, 897-904. doi:10.1016/s0021-9290(03)00071-x

O'Rourke, D., Martelli, S., Bottema, M., Taylor, M., 2016. A computational efficient method to assess the sensitivity of finite-element models: An illustration with the hemipelvis. Journal of Biomechanical Engineering 138, 121008. doi:10.1115/1.4034831

Panagiotopoulou, O., Wilshin, S.D., Rayfield, E.J., Shefelbine, S.J., Hutchinson, J.R., 2014. What makes an accurate and reliable subject-specific finite element model? A case study of an elephant femur. Journal of The Royal Society Interface 9, 351-361. doi: 10.1098/rsif.2011.0323

Pandy, M.G., 2001. Computer modeling and simulation of human movement. Annual Review of Biomedical Engineering 3, 245-273. doi:10.1146/annurev.bioeng.3.1.245

Pandy, M.G., Zajac, F.E., 1991. Optimal muscular coordination strategies for jumping. Journal of Biomechanics 24, 1-10. doi:10.1016/0021-9290(91)90321-d

Pauchard, Y., Fitze, T., Browarnik, D., Eskandari, A., Pauchard, I., Enns-Bray, W., Pálsson, H., Sigurdsson, S., Ferguson, S.J., Harris, T.B., Gudnason, V., Helgason, B., 2016. Interactive graph-cut segmentation for fast creation of finite element models from clinical ct data for hip fracture prediction. Computer Methods in Biomechanics and Biomedical Engineering 19, 1693-1703. doi:10.1080/10255842.2016.1181173

Pawlak, Z., Urbaniak, W., Hagner-Derengowska, M., Hagner, W., 2015. The Probable explanation for the low friction of natural joints. Cell Biochemistry and Biophysics 71, 1615-1621. doi:10.1007/s12013-014-0384-8

Phillips, A.T., Villette, C.C., Modenese, L., 2015. Femoral bone mesoscale structural architecture prediction using musculoskeletal and finite element modelling. International Biomechanics 2, 43-61. doi:10.1080/23335432.2015.1017609

Pizzolato, C., Reggiani, M., Saxby, D.J., Ceseracciu, E., Modenese, L., Lloyd, D.G., 2017. Biofeedback for gait retraining based on real-time estimation of tibiofemoral joint contact forces. IEEE Transactions on Neural Systems and Rehabilitation Engineering 25, 1612-1621. doi:10.1109/tnsre.2017.2683488

Schileo, E., Taddei, F., Malandrino, A., Cristofolini, L., Viceconti, M., 2007. Subject-specific finite element models can accurately predict strain levels in long bones. Journal of Biomechanics 40, 2982-2989. doi:10.1016/j.jbiomech.2007.02.010

Seeger, M., 2004. Gaussian processes for machine learning. International Journal of Neural Systems 14, 69-106. doi:10.1142/s0129065704001899

Taylor, M., Perilli, E., Martelli, S., 2017. Development of a surrogate model based on patient weight, bone mass and geometry to predict femoral neck strains and fracture loads. Journal of Biomechanics 55, 121-127. doi:10.1016/j.jbiomech.2017.02.022

Taylor, M., Prendergast, P.J., 2015. Four decades of finite element analysis of orthopaedic devices: Where are we now and what are the opportunities? Journal of Biomechanics 48, 767-778. doi:10.1016/j.jbiomech.2014.12.019

Tu, J.V., 1996. Advantages and disadvantages of using artificial neural networks versus logistic regression for predicting medical outcomes. Journal of Clinical Epidemiology 49, 1225-1231. doi:10.1016/s0895-4356(96)00002-9

Walter, J.P., Pandy, M.G., 2017. Dynamic simulation of knee-joint loading during gait using force-feedback control and surrogate contact modelling. Medical Engineering & Physics 48, 196-205. doi:10.1016/j.medengphy.2017.06.043

Wang, C., Duan, Q., Gong, W., Ye, A., Di, Z., Miao, C., 2014. An evaluation of adaptive surrogate modeling based optimization with two benchmark problems. Environmental Modelling & Software 60, 167-179. doi:10.1016/j.envsoft.2014.05.026

Wang, G.G., Shan, S., 2007. Review of Metamodeling Techniques in Support of Engineering Design Optimization. Journal of Mechanical Design 129, 370-380. doi:10.1115/1.2429697

Younes, L.B., Nakajima, Y., Saito, T., 2014. Fully automatic segmentation of the femur from 3D-CT images using primitive shape recognition and statistical shape models. International Journal of Computer Assisted Radiology and Surgery 9, 189-196. doi:10.1007/s11548-013-0950-3

Zhou, J.-J., Zhao, M., Liu, D., Liu, H.-Y., Du, C.-F., 2017. Biomechanical property of a newly designed assembly locking compression plate: Three-dimensional finite element analysis. Journal of Healthcare Engineering, Article ID: 8590251. doi:10.1155/2017/8590251

Ziaeipoor, H., Martelli, S., Pandy, M., Taylor, M., 2018. Efficacy and efficiency of multivariate linear regression for rapid prediction of femoral strain fields during activity. Medical Engineering & Physics, (In press). doi:10.1016/j.medengphy.2018.12.001

Figure 1

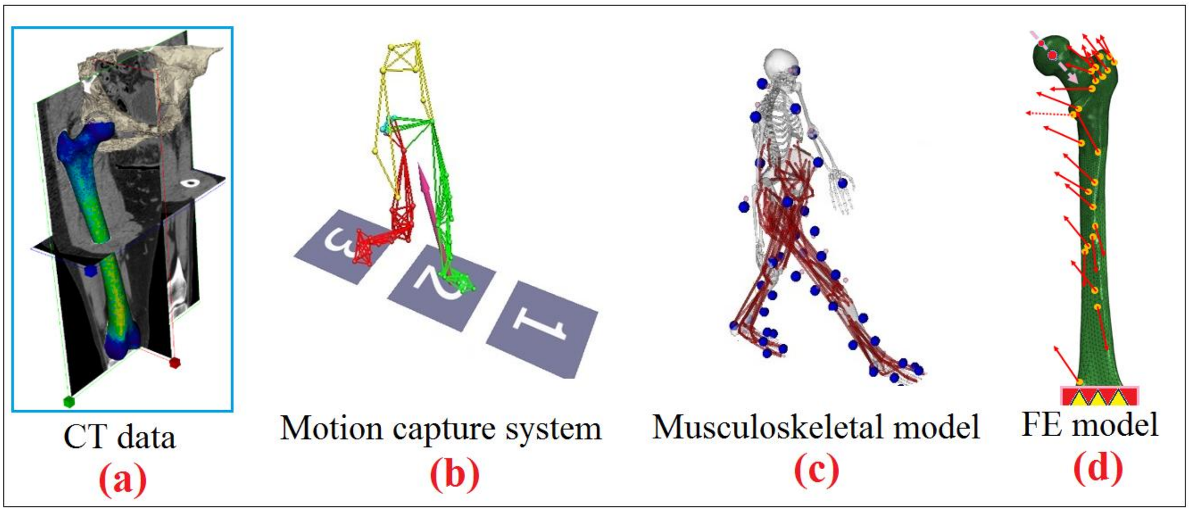

3
2
1
CT data
(a)
Motion capture system
(b)
Musculoskeletal model
(c)
FE model
(d)

Figure 2

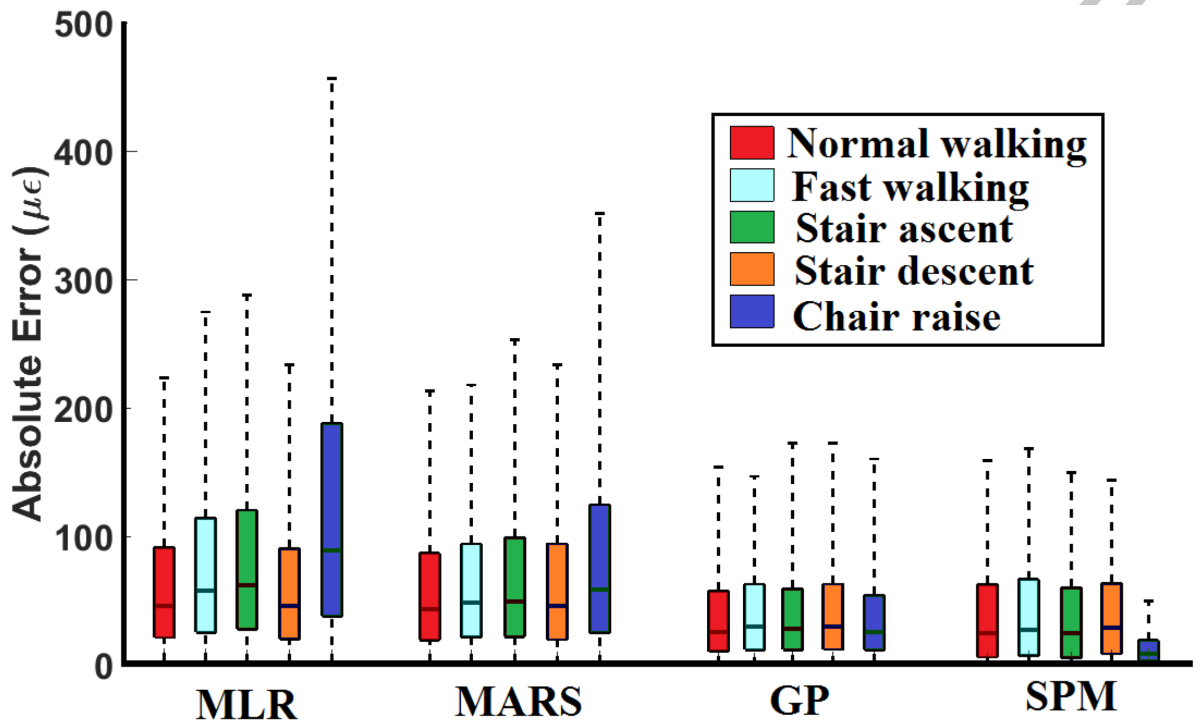
Absolute Error ($\mu\epsilon$)
0
100
200
300
400
500
Normal walking
Fast walking
Stair ascent
Stair descent
Chair raise
MLR
MARS
GP
SPM

Figure 3

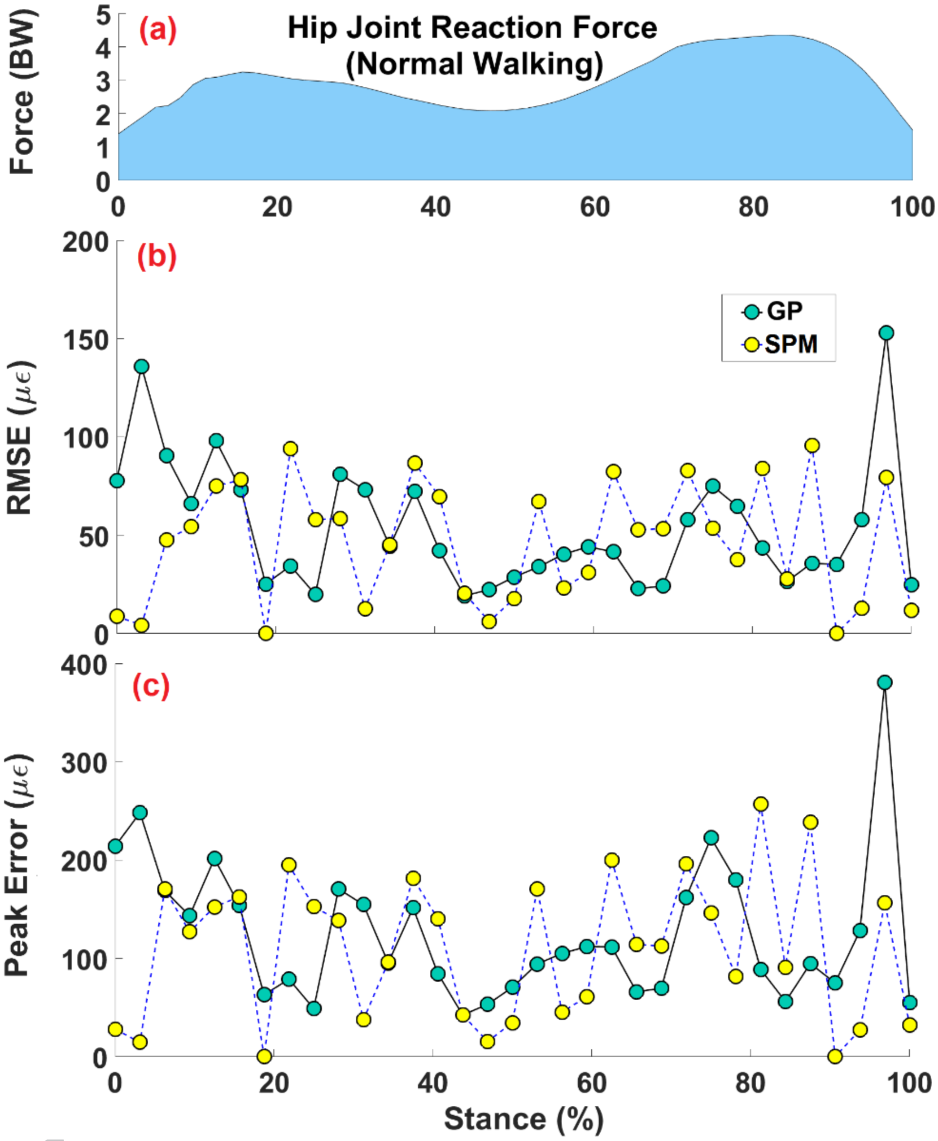

Force (BW)
(a)
Hip Joint Reaction Force
(Normal Walking)
(b)
RMSE ($\mu\epsilon$)
GP
SPM
(c)
Peak Error ($\mu\epsilon$)
Stance (%)

Figure 4

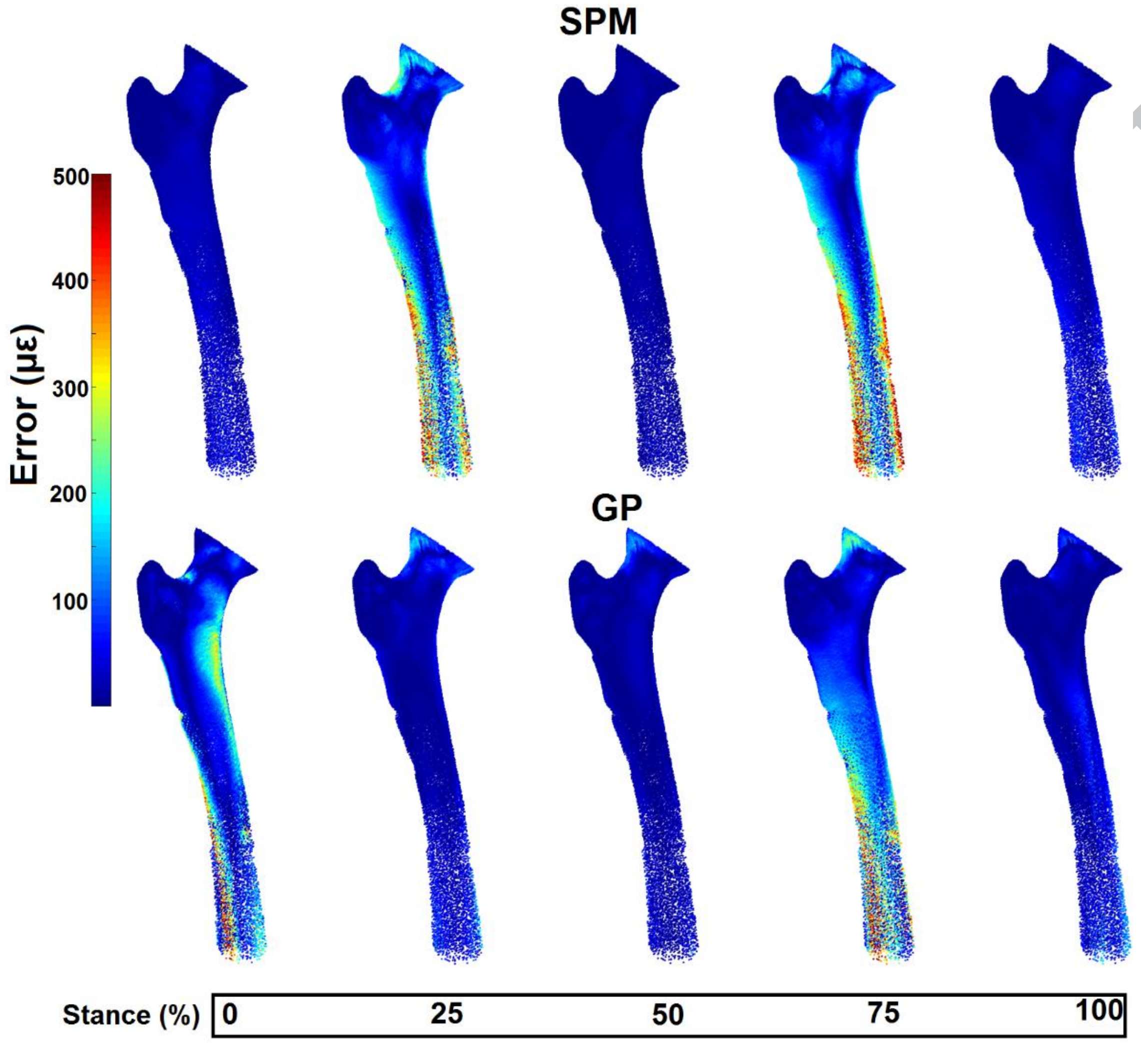

Figure 5

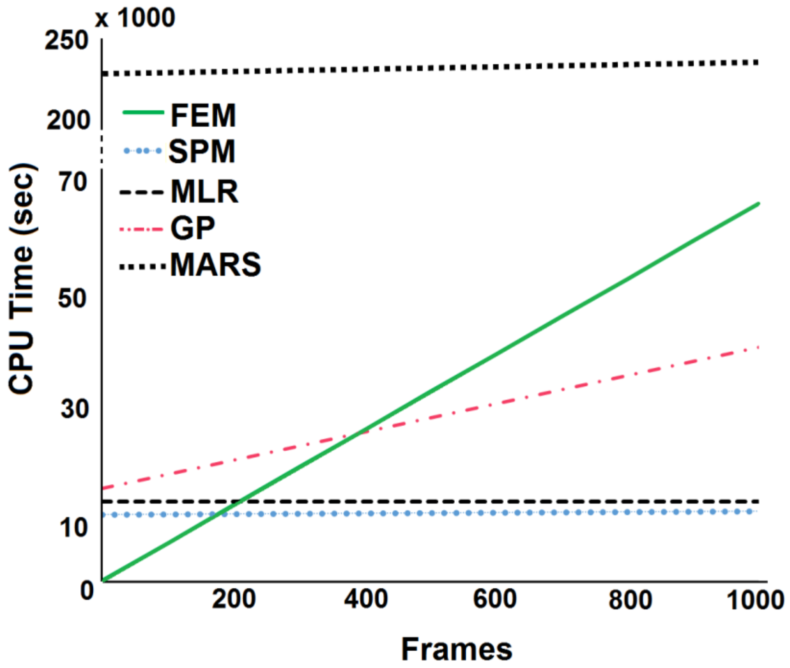

x 1000
250
200
70
50
30
10
0
CPU Time (sec)
FEM
SPM
MLR
GP
MARS
200
400
600
800
1000
Frames

Figure captions

Figure 1. From the left hand side the CT images and superimposed the young modulus map in the finite-element model of the femur, a schematic representation of the motion capture experiment (b), the musculoskeletal model used for computing muscle and joint reaction forces (c) and, a schematic representation of the FE model and its boundary conditions (d). Muscle forces (red arrows), muscle attachment points (orange circles), hip reaction force and point of application (pink dashed line and small red circle), femoral head centre (red circle) and distal constraint (red triangles) are displayed.

Figure 2. The strain error (median, 50th percentile and range) calculated for the different methods (MLR, MARS, GP, SPM) for each activity separately.

Figure 3. Comparison of the strain error in the SPM and GP methods for normal walking. Hip contact force during stance (a), frame-by-frame root mean square error (RMSE) (b), and peak error (c). Forces are expressed in body weight (BW). The femoral head was removed to minimize the localized effect of the point load representing the hip contact force applied to the femoral head.

Figure 4. Error distribution in the SPM (top) and GP (bottom) methods for the stance phase of normal walking.

Figure 5. Total CPU time required by the full finite-element analysis and for model construction (i.e., solving 200 finite-element analysis and training) and predicting femoral strain using MLR, MARS and GP.

Tables

Table 1. Mean and peak error for the different surrogate modelling methods (Multivariate Linear Regression (MLR), Multivariate Adaptive Regression Splines (MARS) and Gaussian Process (GP)) for increasing training set and different sampling methods, including Latin hypercube (LH) sampling and Design of Experiment (DOE). These reported errors are based on pooled data.

Training dataset	Methods	LH			DOE		
		Peak error$_{All}$	$RMSE_{All}$ (mean)	Training time (h)	Peak error$_{All}$	$RMSE_{All}$ (mean)	Training time (h)
50	MLR	1,082,306	227,315	0.14	911	134	0.14
	MARS	1,234,000	9,348,000	6.8	851	187	6.9
	GP	674	111	0.2	495	91	0.2
100	MLR	1021	132	0.14	697	109	0.14
	MARS	1422	508	23.0	678	133	22.7
	GP	461	75	0.3	556	83	0.3
200	MLR	540	108	0.15	521	99	0.15
	MARS	785	170	60.8	414	100	59.7
	GP	519	73	0.9	316	53	0.8
300	MLR	537	107	0.15	493	94	0.15
	MARS	441	106	93.5	385	90	91.7
	GP	528	62	2.9	280	46	2.1

*One processor used for training MARS and four processors used for MLR and GP